Am J Cancer Res 2026;16(10):4355-4370
www.ajcr.us /ISSN:2156-6976/ajcr0167101

Original Article

Paraptosis indicted by Calpeptin is due to CHAC1 mediated glutathione degradation in glioma cells

Yuxue Sun[1,2,3], Yong Chen[3], Haiyan Huang[3], Zhixin Zhan[3], Chaochao Zhang[3], Jiacheng Lai[3], Chaoyue Li[1,2], Ziqiang Liu[1,2,3]

[1]Henan Provincial People's Hospital, Cerebrovascular Disease Hospital, People's Hospital of Zhengzhou University, Zhengzhou 450003, Henan, China; [2]Henan Provincial People's Hospital, Cerebrovascular Disease Hospital, People's Hospital of Henan University, Zhengzhou 450003, Henan, China; [3]Department of Neurosurgery, The First Hospital of Jilin University, Changchun 130021, Jilin, China

Received June 28, 2025; Accepted October 13, 2026; Epub October 15, 2026; Published October 30, 2026

Abstract: Glioma is the most common form of malignant tumor of the central nervous system and has a poor prognosis. This study aimed to determine whether calpeptin (CP), an inhibitor of calpains, induces paraptosis in glioma cells, involving programmed cell death independent of caspase activation. We found that CP induced vacuole formation in the cytoplasm of T98G and LN18 glioma cells. An endoplasmic reticulum (ER) fluorescent probe showed that vacuole formation was due to ER swelling. CP induced ER stress and mitochondrial dysfunction, causing increased production of reactive oxygen species (ROS) and inhibition of mitochondrial membrane potential with activation of the PARP1 and MAPK signaling pathways. The oxygen consumption rate assay (OCR) showed that CP reduced mitochondrial oxidative phosphorylation in T98G cells. Furthermore, CP caused the release of Ca^{2+} in the ER of glioma cells into the cytoplasm and destroyed intracellular Ca^{2+} homeostasis. However, the ER stress inhibitor 4-PBA, the antioxidant N-acetylcysteine, the PARP-1 inhibitor benzamide, the MAPK inhibitors U0126, SP600125 and SB203580, and the Ca^{2+} inhibitor 2-APB did not block CP-induced paraptosis. Finally, we found that the addition of glutathione (GSH) to the medium blocked CP-induced paraptosis. By sequencing the transcriptome, we identified CHAC1 as a key factor involved in GSH metabolism that was significantly up-regulated by CP. Knocking out CHAC1 prevented CP-induced paraptosis, and we concluded that glutathione degradation caused by CHAC1 up-regulation is the crucial mechanism underlying CP-induced paraptosis. Taken together, our findings provide novel insights into the treatment of gliomas through paraptosis induced by CP.

Keywords: Calpeptin, paraptosis, CHAC1, glutathione, endoplasmic reticulum stress

Introduction

Glioma has high recurrence and mortality rate [1]. In 2020, approximately 308,102 new cases of glioma were reported, and 251,329 new glioma-related deaths occurred worldwide [2]. Glioblastoma is the most malignant form, accounting for approximately 45% of all gliomas, and the relative five-year survival rate is only approximately 5% [3, 4]. Current treatment methods for glioma include surgery, radiation therapy, chemotherapy and immunotherapy. However, the survival rate for patients with glioma has not improved significantly [5]. Temozolomide (TMZ) is currently the first choice of postoperative chemotherapy for gliomas. Developing drug resistance is reported to be due to the heterogeneity of gliomas [6]. For that reason, the development of new antiglioma drugs with new mechanisms is essential.

In 2000, Sperandio et al. first described paraptosis as programmed cell death that clearly differed from apoptosis regarding cell morphology and biochemistry [7]. Paraptosis is not involved in the caspase system and is insensitive to apoptosis inhibitors. Its typical characteristics are wide vacuoles in the cytoplasm and dilation of the ER and/or mitochondria [8]. The protein synthesis inhibitor cycloheximide (CHX) has been shown to inhibit paraptosis [9]. MAPK family members are involved in the paraptotic process [10]. Furthermore, an association has been reported between paraptosis, the destruc-

tion of intracellular calcium homeostasis and mitochondrial dysfunction [11]. Recently, a study found that an imbalance in the GSH system induced an increase in reactive oxygen species (ROS) in cells and participated in the paraptosis process [12]. The cation transport regulator homolog-1 (CHAC1) was first identified in 2006 in a group of homologous genes rich in the arm component of the unfolded protein response (UPR) pathway-activating transcription factor 4 (ATF4) [13]. CHAC1 is involved in endoplasmic reticulum stress and is the downstream signaling molecule of ATF4 [14]. In addition, CHAC1 is also involved in GSH metabolism and can specifically catabolise GSH into 5-oxo-L-proline and Cys-Gly dipeptide, which is a key molecule in the GSH metabolic pathway [15]. Several recent studies have confirmed that CHAC1-mediated GSH depletion is involved in the process of apoptosis and ferroptosis [16-18], but its role in paraptosis remains unclear.

Calpeptin (CP), an inhibitor of calpains, could inhibit the proliferation of pancreatic cancer cells by disrupting cancer-stromal interactions [19]. CP can also cause cell cycle arrest, promote apoptosis, and inhibit cell invasion in various cancers [20-22]. However, the ability of CP to induce paraptosis in cancer cells is unclear. This study aimed to determine whether CP-related targeting of the GSH system causes ER stress and mitochondrial dysfunction, therefore inducing paraptosis in glioma cells.

Materials and methods

Reagents and antibodies

CP (purity > 97%) was purchased from Selleck (Houston, USA), and its chemical structure is shown in **Figure 1A**. 4-Phenylbutyric acid (4-PBA) and 2-aminoethyl diphenylborinate (2-APB) were purchased from Selleck (Houston, USA). Cycloheximide (CHX) was purchased from MCE (New Jersey, USA). U0126, SP600125, SB203580, and benzamide were purchased from TargetMol (Shanghai, China). GSH, Z-VAD-FMK, N-acetylcysteine (NAC), cell counting kit-8(CCK-8), cell cycle and apoptosis analysis kits, mitochondrial permeability transition pore (mPTP) assay kits, Fluo-3 AM, ROS assay kits, MitoTracker Green, ER-Tracker Red and GreenNuc™ caspase-3 assay kits for live cells were purchased from Beyotime (Shanghai, China). A microreduced glutathione (GSH) assay kit was purchased from Solarbio (Beijing, China). A JC-10 mitochondrial membrane potential assay kit was purchased from Yeasen (Shanghai, China). Dulbecco's modified Eagle's medium (DMEM) was purchased from Gibco (NY, USA). Fetal bovine serum (FBS) and penicillin-streptomycin solution were purchased from Biological Industries (Israel). Nanoscale micropoly Transfection Reagent (Namipo) and siRNA were purchased from TranSheep (Shanghai, China). Rabbit anti-human cyclin B1 (1:5000), PARP1 (1:1000), cleaved-PARP1 (c-PARP1) (1:2000), p-P38 (1:1000), pro-caspase 3 (1:1000), cleaved caspase 3 (1:500), cleaved caspase 9 (1:2000), and Bax (1:2000) polyclonal antibodies were purchased from Abcam (Cambridge, MA, USA). Rabbit anti-human Alix (1:5000), ATF4 (1:2000), CHOP (1:2000), CHAC1 (1:2000), p-ERK (1:2000), and p-JNK (1:2000) polyclonal antibodies were purchased from Proteintech (Wuhan, China). Mouse anti-human GAPDH (1:5000) polyclonal antibodies were purchased from Engibody (DE, USA). Goat anti-mouse IgG (1:5000) and goat anti-rabbit IgG (1:5000) polyclonal antibodies were purchased from Yeasen (Shanghai, China).

Cell culture

T98G and LN18 human glioblastoma cell lines were purchased from the American Type Culture Collection (Manassas, VA, USA). Cells were cultured in DMEM, supplemented with 10% FBS and 1% penicillin-streptomycin solution, and placed in a cell incubator at 37°C and 5% CO_2.

Cytotoxicity assay

Ninety-six well plates were seeded with T98G and LN18 cells at a density of 1×10^3 cells/well. Twenty-four hours after cell seeding, the old medium was replaced with 100 μL of complete medium containing CP, Z-VAD-FMK, CHX, NAC, GSH, 4-PBA, 2-APB, benzamide, 3-MA, U0126, SP600125 and SB203580. After incubation for an additional 24 hours, 10 μL of CCK-8 solution was added to each well. After incubation at 37°C for 1 hour, absorbance was measured at a wavelength of 450 nm.

Cell cycle analysis

After treatment of T98G and LN18 cells with CP for 6 hours, cells were digested with trypsin, fixed overnight in 70% precooled ethanol at

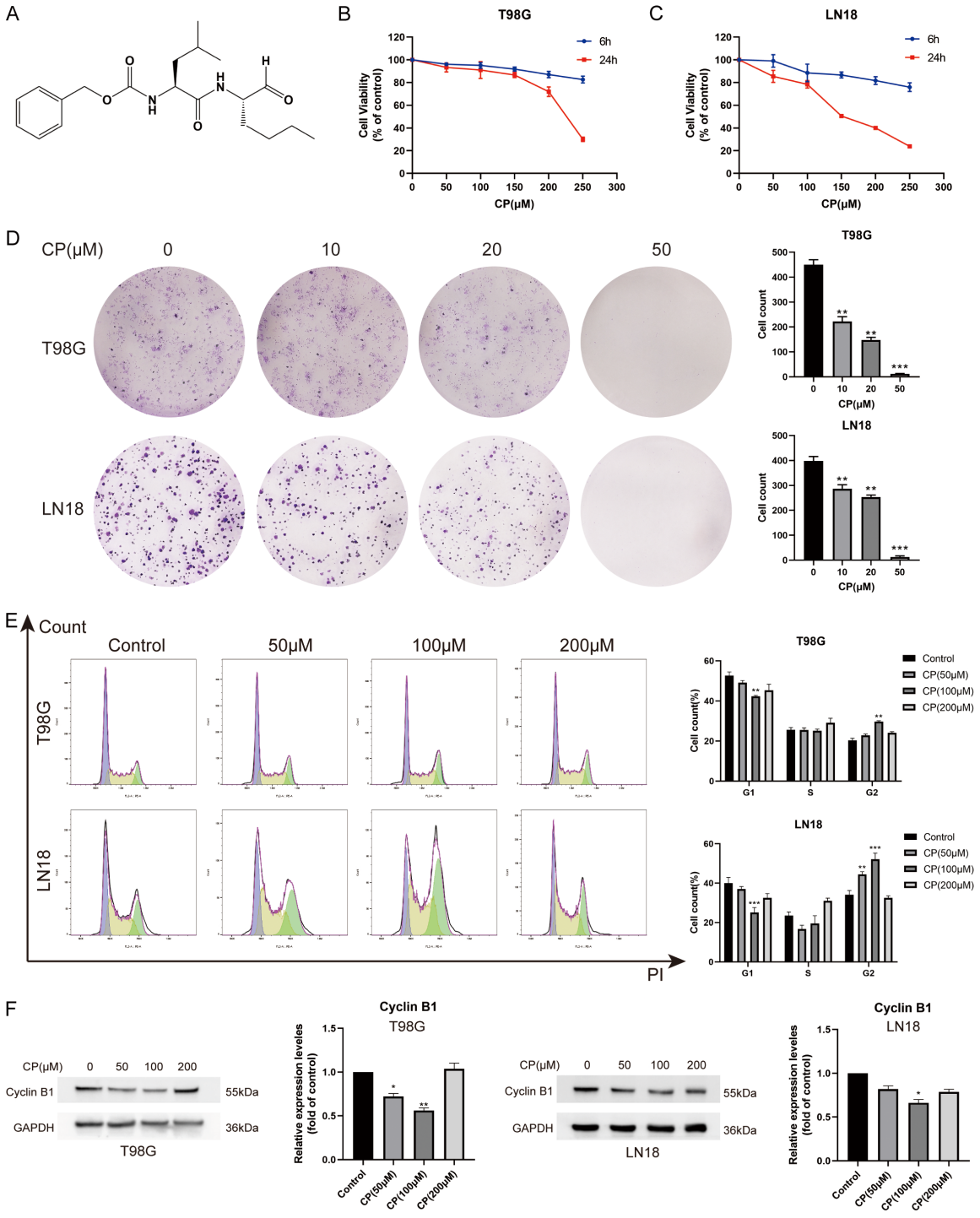

Figure 1. CP inhibited glioma cell proliferation. A. The chemical structure of CP. B and C. Cytotoxicity of CP to T98G cells and LN18 cells. Cells were treated with different concentrations of CP for 6-24 h, and alive cells was measured by CCK-8 assay. D. CP inhibited clony formation in T98G and LN18 cells. The colonies were counted using the ImajeJ software (**P < 0.01, ***P < 0.001). E and F. Effects of CP on the cell cycle of T98G and LN18 cells. Cells were treated with different concentrations of CP for 6 h (*P < 0.05, **P < 0.01, P < 0.001).

-20°C, washed with PBS, and incubated for 20 min with propidium iodide (PI) and RNA enzyme, and cell cycles were analyzed by flow cytometry.

Cell apoptosis analysis

For 24 hours, 2×10^5 cells were inoculated into 6-well plates. Cells were collected after 6 hours of treatment with different concentrations of CP. The collected cells were incubated with Annexin V-FITC and PI buffer for 20 min, and apoptotic cells were identified by flow cytometry.

Caspase-3 activity assay

After 6 hours of treatment with different CP concentrations, T98G and LN18 cells were collected. GreenNuc caspase-3 substrate was added to the cell suspension at a final concentration of 5 μM. Caspase-3 activity was analyzed by flow cytometry after incubation for 20 min at room temperature.

mPTP assay

After 6 hours of treatment with CP, T98G and LN18 cells were collected. The cell suspension was incubated with Calcein-AM staining solution and $CoCl_2$ at 37°C for 30 min. After centrifugation, cells were resuspended in detection buffer, and mPTP was measured by flow cytometry.

Transmission electron microscopy (TEM)

T98G cells were fixed with 2.5% glutaraldehyde for two days. After washing with 0.1 M phosphate buffer (pH 7.4) for 45 min, cells were fixed with 1% osmium tetroxide for 2 hours. After dehydration with a gradient of ethanol and acetone, the cells were embedded in epoxy resin. Finally, the epoxy sections were cut at 60 nm, attached to a 100 mesh grid, stained with uranyl acetate and lead citrate and observed under a transmission electron microscope.

Western blotting

After treating T98G and LN18 cells with CP for 6 hours, cells were collected and then centrifuged at 12000×g for 30 min at 4°C. Cell lysates were mixed with SDS-PAGE loading buffer (Dingguo, China) and boiled at 100°C for 10 min. Protein samples were electrophoresed on an SDS-PAGE gel, transferred to a PVDF membrane, and blocked in 5% skimmed milk powder for 1 hour at room temperature. The primary antibody was incubated overnight at 4°C, the secondary antibody was incubated at room temperature for 1 hour, and then the blots were developed using an ECL kit (Yeasen, China). Each Western blot was repeated three times, and each protein level was normalized to the GAPDH protein level.

Mitochondrial and ER staining

After treating glioma cells with CP for 6 hours, the cell culture medium was removed, and a working solution containing ER-Tracker Red or MitoTracker Green was added and incubated at 37°C for 30 min. After the cells were washed twice with DMEM, the ER and mitochondria were observed by fluorescence microscopy.

Measurement of ROS

Cells were seeded in 6-well plates at a density of 1×10^5 cells per well for 24 hours, and then treated with CP for 6 hours. The DCFH-DA fluorescent probe was incubated with cells at 37°C for 20 min after dilution in cell culture medium at 1:1000. After the cells were washed with cell culture medium three times, intracellular ROS levels were observed under fluorescence microscopy.

Mitochondrial membrane potential (ΔΨm) assay

After treating T98G and LN18 cells with CP for 6 hours, cells were collected and incubated in JC-10 staining solution at 37°C for 20 min. Cells were then washed twice with JC-10 buffer and mitochondrial membrane potential was detected by flow cytometry.

Oxygen consumption rate (OCR) assay

The evaluation of mitochondrial oxidative phosphorylation of glioma cells used OCR, and subsequently T98G cells were seeded on XF 96 well plates at a density of 1×10^4 cells/well. After the cells were treated with CP for 6 hours, the OCR was monitored in real time using an XFe96 extracellular flow analyzer. During measurement, the ATP synthase inhibitor oligomycin, the FCCP uncoupling agent, and the electron transport inhibitor antimycin A were sequentially added to a 96-well plate.

Measurement of intracellular Ca^{2+}

Fluo-3 AM was used to measure the intracellular Ca^{2+} concentration. After T98G and LN18 cells were treated with CP for 6 hours, the cells were collected and incubated with Fluo-3

Table 1. Sequence information of siRNA NC and siCHAC1

siRNA sequences	Sense	Antisense
siRNA NC	UUCUCCGAACGUGUCACGUTT	ACGUGACACGUUCGGAGAATT
siCHAC1#1	GACGCUCCUUGAAGAUCAUTT	AUGAUCUUCAAGGAGCGUCTT
siCHAC1#2	GCCACAACCUUGAAUACUUTT	AAGUAUUCAAGGUUGUGGCTT
siCHAC1#3	CGUGGCAUACCAAGUGCAATT	UUGCACUUGGUAUGCCACGTT

AM for 30 min at 37°C. The cells were then washed three times with PBS and the fluorescence intensity was measured using flow cytometry.

Analysis of cellular GSH

After 6 hours of CP treatment, the cells were digested and collected with trypsin, and washed twice with precooled PBS. According to the manufacturer's instructions, a GSH assay kit was used to measure the GSH content in glioma cells.

Transfection of siRNA

T98G cells were seeded in 6-well plates at a density of 2×10^5 cells/well. siRNA transfection was performed overnight. The siRNA sequences were shown in **Table 1**. The siRNA and Namipo were mixed at a 1:1 ratio and incubated at room temperature for 10 minutes, before being added to the cell culture medium to give a final siRNA concentration of 100 nM. The cell culture medium was changed after 16 hours of transfection and the transfection efficiency was observed under a fluorescence microscope. The protein was extracted after 48 hours of transfection for the experiment.

Statistical analysis

Each experiment was repeated three times and the results are shown as the mean ± SD. Statistical data were analyzed using GraphPad Prism software (version 8.0; San Diego, CA, USA) and Repeat measurement ANOVA. Statistical significance was established at $P < 0.05$.

Results

The proliferation of human glioma cells was inhibited by CP

After incubating T98G and LN18 cells with different concentrations of CP for 6-24 hours, the cytotoxicity of CP was measured using CCK-8. We found that with increasing concentration and prolonged incubation time, the cytotoxicity of CP to glioma cells gradually increased and LN18 cells were more sensitive to CP than T98G cells (**Figure 1B** and **1C**). The clone formation experiment further confirmed that CP inhibited glioma cell proliferation (**Figure 1D**). The cell cycle was then analyzed by flow cytometry and Western blotting. Interestingly, low concentrations of CP caused G2/M phase arrest in glioma cells, while high concentrations of CP did not cause cell cycle arrest (**Figure 1E**). Cyclin B is a protein that regulates the G2/M phase of the cell cycle. Therefore, we used Western blotting to detect the content change of cyclin B protein, and the results were the same as those obtained by flow cytometry (**Figure 1F**). These results showed that cell cycle arrest cannot be the main way that CP inhibits the proliferation of glioma cells.

In glioma cells, CP caused non-apoptotic cell death

Previous studies have shown that CP induces apoptosis in other cancer cells [20-22]. Although flow cytometry showed that CP increased the proportion of Annexin V-FITC and PI positive cells in T98G and LN18 cell lines (**Figure 2A**), there was no significant change in caspase 3 activity in T98G and LN18 cells (**Figure 2B**). Western blot analysis also showed that CP did not increase cleaved-caspase 3 and cleaved-caspase 9 levels in glioma cells. In contrast, CP inhibited the expression of the proapoptotic protein Bax (**Figure 2C**). Next, we compared the effect of the apoptosis-inducing compound CCCP (50 μM) with CP (200 μM) in glioma cells. Western blot analysis showed that CP (200 μM) had no significant effect on the intracellular levels of pro-caspase 3 and cleaved-caspase 3. However, CCCP (50 μM) significantly reduced the content of pro-caspase 3 and activated cleaved-caspase 3 (**Figure 2D**). In apoptotic cells, the degree of opening of mPTP tended to increase, which was shown as decreased green fluorescence using the mPTP assay kit. Interestingly, flow cytometry results showed that CP increased

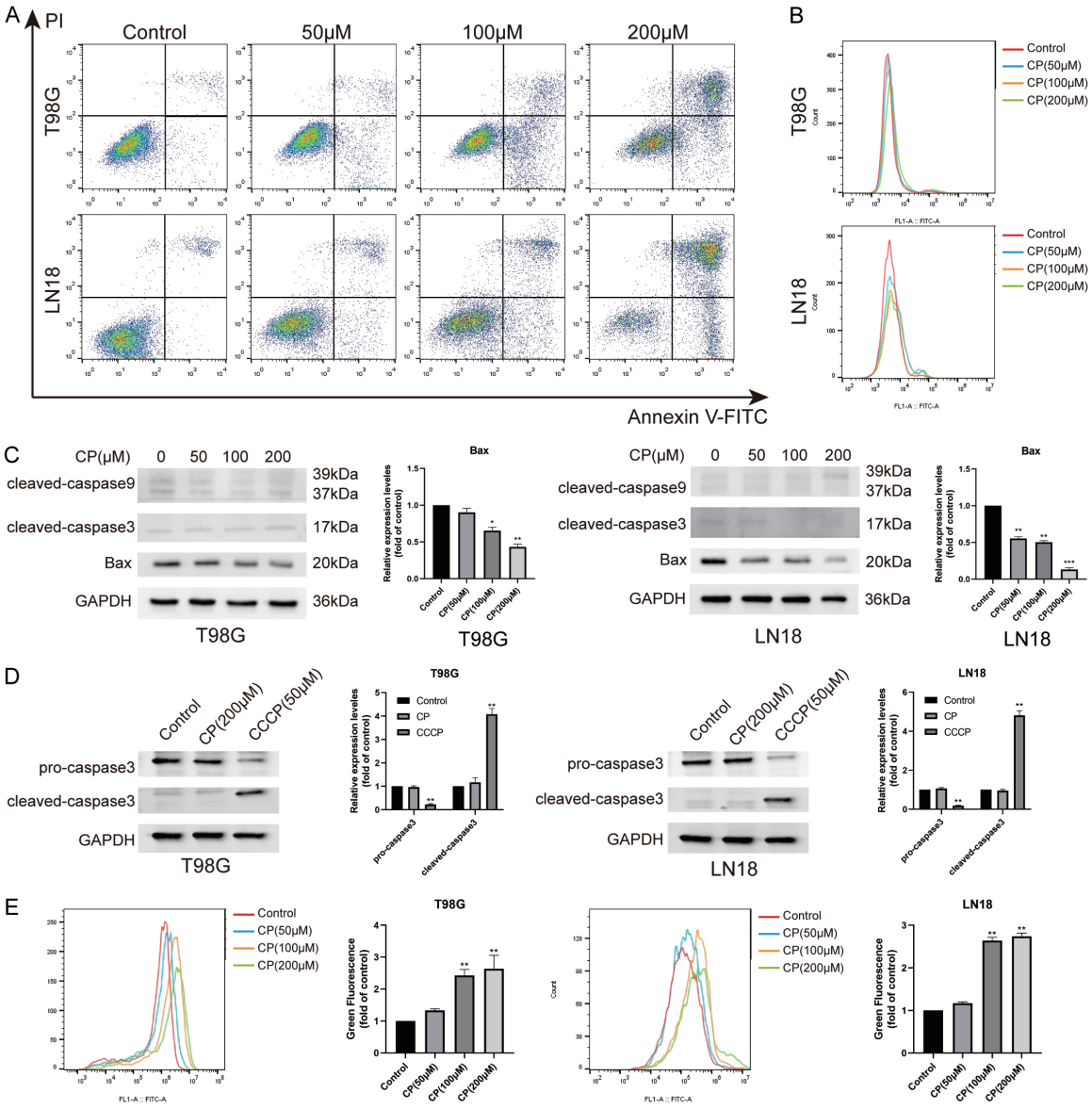

Figure 2. CP caused non-apoptotic cell death in glioma cells. A. T98G and LN18 cells were treated with different concentrations of CP for 6 h. An apoptosis kit was used to detect the ratio of Annexin V-FITC and PI positive cells. B. T98G and LN18 cells were treated with different concentrations of CP for 6 h. GreenNuc™ caspase-3 assay kit was used to detect the effect of CP on caspase-3 activity. C. Western blotting was used to detect the changes in apoptotic proteins in glioma cells treated with CP for 6 h (*P < 0.05, **P < 0.01, ***P < 0.001). D. Changes in intracellular apoptotic proteins after glioma cells were treated with CP and the apoptosis-inducing compound CCCP (**P < 0.01). E. Changes in mPTP after 6 h of treatment with CP in glioma cells (**P < 0.01).

green fluorescence in glioma cells; that is, CP decreased the degree of mPTP opening (**Figure 2E**). These results indicated that CP causes nonapoptotic cell death in glioma cells.

Paraptosis in glioma cells was induced by CP

Paraptosis is distinct from apoptosis and is characterized by extensive vacuolation within cells that require protein synthesis [8]. Z-VAD-FMK could not prevent paraptosis, while the protein synthesis inhibitor CHX could attenuate paraptosis [23]. In this study, we found that CP induced the formation of many vacuoles in glioma cells, and that Z-VAD-FMK could not block the formation of vacuoles induced by CP, while the addition of CHX significantly inhibited the generation of intracellular vacuoles induced by CP (**Figure 3A**). However, the CCK-8 results showed that Z-VAD-FMK and CHX did not sal-

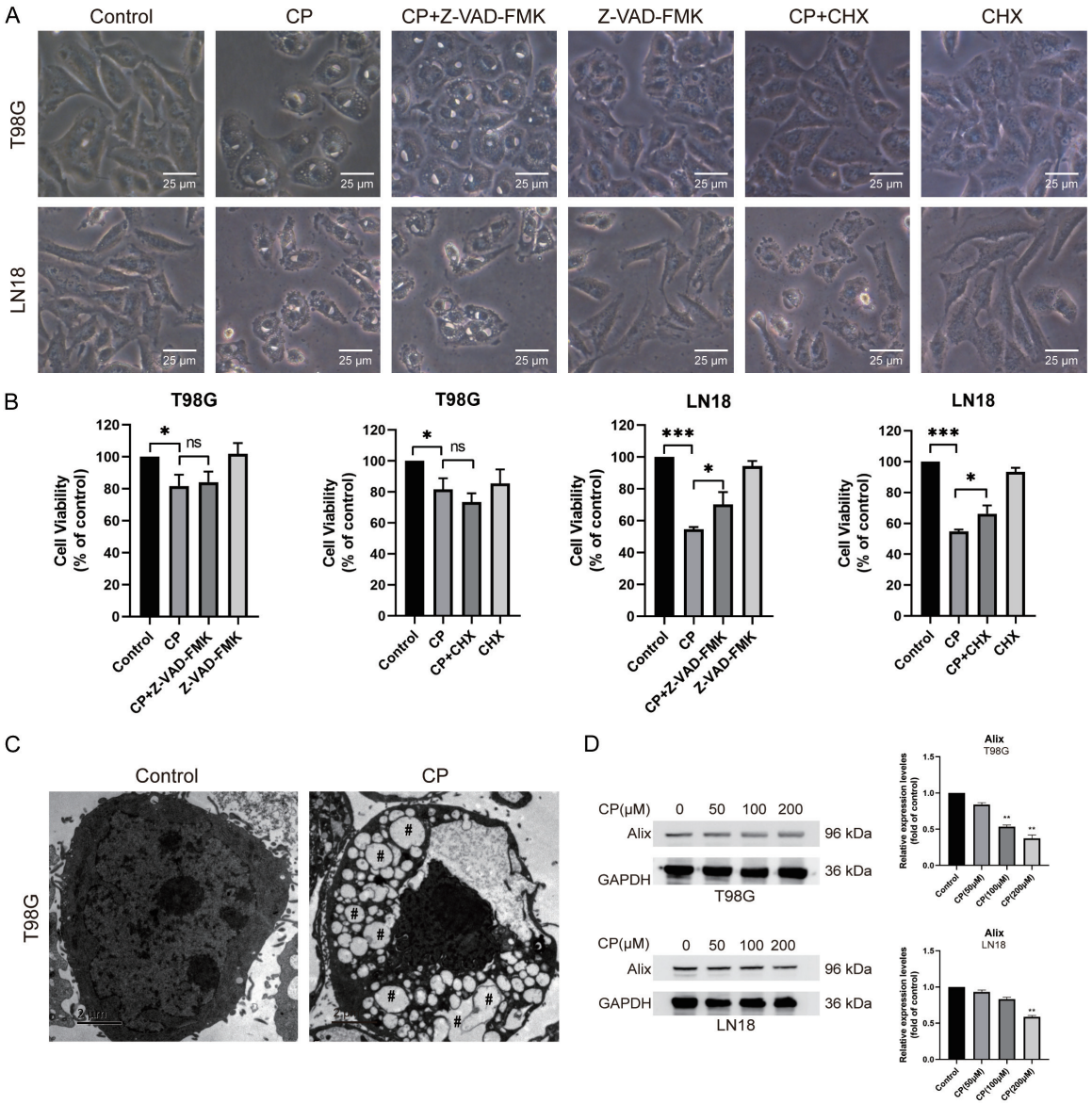

Figure 3. CP induced paraptosis in glioma cells. A. Microscope images of CP-treated glioma cells. Glioma cells were pretreated with Z-VAD-FMK (20 μM) and CHX (20 μM), and then treated with CP (200 μM) for 6 h. B. The effect of Z-VAD-FMK and CHX on the viability of CP-induced paraptosis. Cells were pretreated with Z-VAD-FMK (20 μM) and CHX (20 μM), and then treated with CP (200 μM) for 24 h. The alive cells were measured with a CCK-8 assay ($^{*}P < 0.05$, $^{***}P < 0.001$). C. T98G cells were treated with CP (200 μM) for 6 h and then analyzed by transmission electron microscopy. # shows swollen ER. Scale bars are 2 μm. D. Western blot analysis of Alix protein changes. Cells were treated with various doses of CP for 6 h ($^{**}P < 0.01$).

vage CP-induced T98G cell death but decreased cytotoxicity to LN18 cells (**Figure 3B**). TEM analysis showed that intracellular vacuoles were produced due to swelling of the ER (**Figure 3C**). Furthermore, Alg-2-interacting protein X (Alix) was considered a marker of paraptosis [24], and the Western blot results showed that CP inhibited the expression of the Alix protein (**Figure 3D**). These results indicated that CP induced paraptosis in glioma cells.

Endoplasmic reticular stress was induced in glioma cells by CP

Our labeling of the ER in glioma cells with ER-Tracker Red further indicated that intracellular vacuoles due to CP were derived from swelling of the ER (**Figure 4A**). Furthermore, the Western blot results showed that after CP treatment, the expression levels of two key transcription factors, ATF4 and CHOP, were signifi-

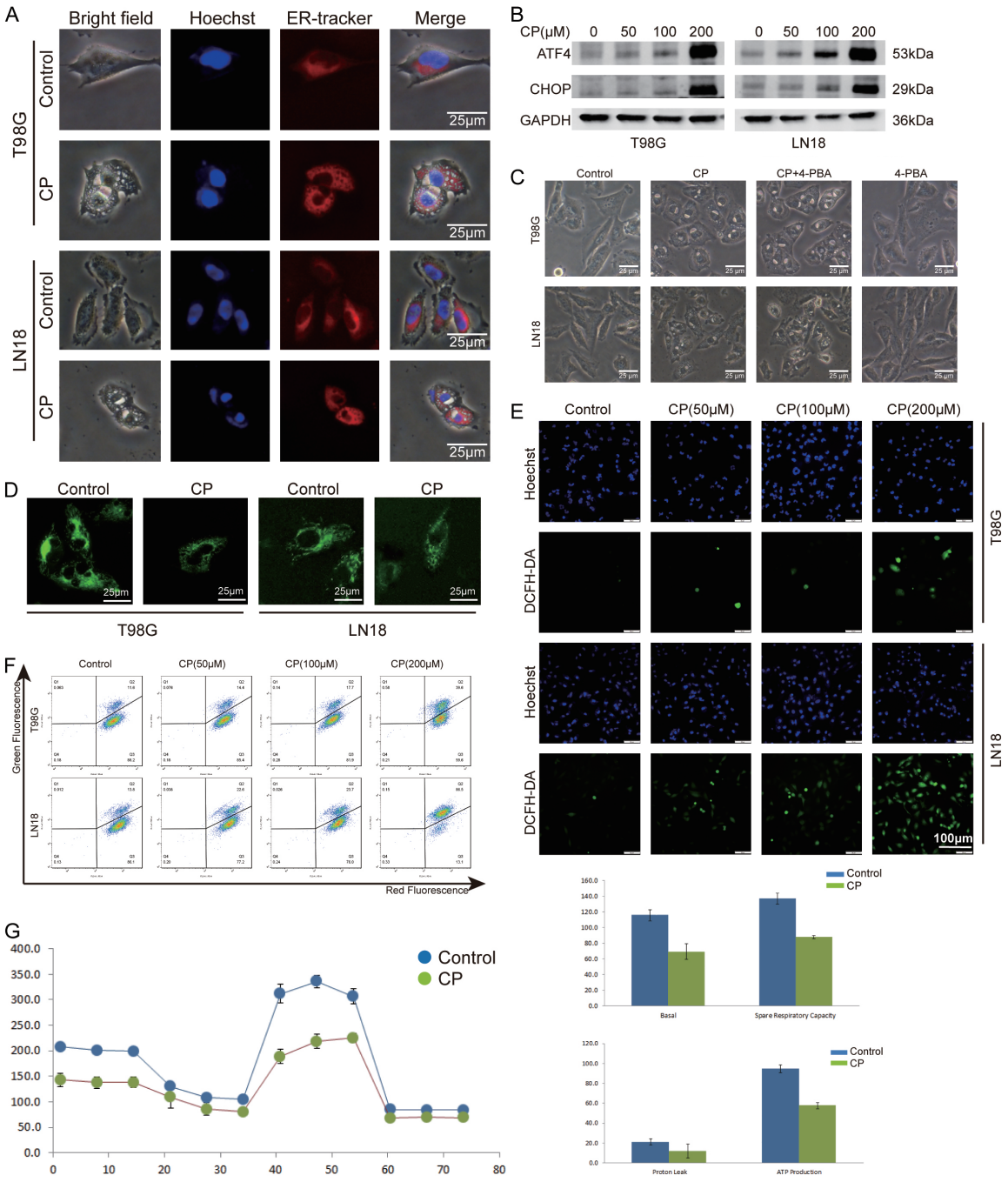

Figure 4. CP induced ER stress and mitochondrial dysfunction in glioma cells. A. Fluorescence image of glioma cells after 6 h of treatment with CP (200 μM). The ER was stained with ER-Tracker red. B. Western blot analysis of the intracellular ER stress proteins ATF4 and CHOP. Cells were treated with different concentrations of CP for 6 h (**P < 0.01, ***P < 0.001). C. Effect of the ER stress inhibitor 4-PBA (2.5 mM) on CP-induced paraptosis. D. Fluorescence image of glioma cells after 6 h of treatment with CP (200 μM). The mitochondrial were stained with Mito-Tracker Green. E. The fluorescent probe DCFH-DA detected the ROS level of glioma cells. Cells were treated with various doses of CP for 6 h. F. JC-10 was used to analyze mitochondrial membrane potential after glioma cells were treated with different concentrations of CP for 6 h. G. The mitochondrial function of T98G cells after 6 h of treatment with CP (200 μM) was detected using a hippocampal XF analyzer. The basal OCR, maximal OCR, proton leak, and ATP production levels are presented.

cantly increased in glioma cells (**Figure 4B**). These results confirmed that CP causes ER stress in glioma cells. However, after using the ER stress inhibitor 4-PBA, we found that 4-PBA

could not block CP-induced paraptosis (**Figure 4C**). Previous studies have shown that many unfolded or misfolded proteins accumulate in the ER during paraptosis, causing ER stress [25-27], which also explains why CHX can attenuate CP-induced paraptosis.

Mitochondrial dysfunction in glioma cells was caused by CP

Various drugs have been reported to induce paraptosis by promoting ROS overproduction and mitochondrial dysfunction in cancer cells [8]. Therefore, we used a mitochondrial fluorescent probe (MitoTracker Green) to detect mitochondrial morphological changes in glioma cells. Fluorescence microscopy showed that the mitochondria of glioma cells treated with CP changed from short rods to dots (**Figure 4D**). The DCFH-DA fluorescent probe showed that CP increased ROS production in glioma cells (**Figure 4E**). The results of the JC-10 kit showed that CP significantly reduced the red/green fluorescence ratio in T98G and LN18 cells, indicating that CP significantly decreased the mitochondrial membrane potential (**Figure 4F**). We also measured the OCR of T98G cells, and the results showed that CP inhibited oxidative phosphorylation (**Figure 4G**). These results confirmed that CP caused mitochondrial dysfunction in glioma cells.

In glioma cells, CP activated the PARP1 and MAPK signaling pathways

In general, it has been recognized that the MAPK pathway participates in paraptosis [28, 29]. Recently, Mir et al. reported that PARP1 is also involved in paraptosis [30]. Therefore, we investigated the effects of CP on the PARP1 and MAPK signaling pathways in glioma cells. Western blot results showed that CP increased the content of the 85k Da and 27k Da molecular weight c-PARP1 (**Figure 5A**). However, the PARP1 inhibitor benzamide was unable to block CP-induced intracellular vacuolation or decrease cytotoxicity compared with the CP-treated group alone (**Figure 5B** and **5C**). In contrast, CP upregulated the expression of p-ERK, p-JNK, and p-P38 in T98G and LN18 cells, activating the MAPK signaling pathway (**Figure 5D**). After the addition of three different MAPK pathway inhibitors, none of the ERK inhibitors, U0126, the JNK inhibitor SP600125, or the P38 inhibitor SB203580, inhibited CP-induced vacuolation or decreased CP cytotoxicity (**Figure 5E** and **5F**).

In glioma cells, Ca^{2+} overload was caused by CP

Intracellular calcium homeostasis is important for maintaining normal cellular function. The ER and mitochondria are the main organelles involved in the storage of calcium ions in cells [31]. ER and mitochondrial stress often destroy the homeostasis of Ca^{2+} in cells and cause Ca^{2+} overload. Intracellular Ca^{2+} overload plays a vital role in paraptosis [32, 33]. Therefore, we investigated the effect of CP on intracellular Ca^{2+} homeostasis using Fluo-3 AM in T98G and LN18 cells. Our results showed that CP significantly increased Ca^{2+} levels in glioma cells (**Figure 5G**). We then added the ER Ca^{2+} release inhibitor 2-APB to treat glioma cells. However, 2-APB did not inhibit CP-induced vacuolation (**Figure 5H**).

Inhibition of the GSH system contributed to CP-induced paraptosis

The GSH system is essential for maintaining redox homeostasis in cells [34]. GSH is distributed mainly in the cytoplasm and a small amount in the nucleus, mitochondria and ER. In addition to ROS scavenging, GSH is also involved in protein folding, DNA synthesis, and intracellular signal transduction [35]. GSH depletion is involved in many cell death processes, including apoptosis, necrosis, ferroptosis, and autophagy [36]. Considering that CP causes destruction of redox homeostasis in glioma cells, we treated glioma cells with the antioxidants NAC and GSH. We found that NAC could neither prevent CP-induced cell vacuoles nor decrease cytotoxicity. GSH blocked intracellular vacuole generation, and significantly decreased the cytotoxicity of CP in glioma cells (**Figure 6A** and **6B**). This finding indicated that inhibition of intracellular ROS production alone could not inhibit CP-induced paraptosis. We found that CP reduced intracellular GSH levels in T98G and LN18 cells (**Figure 6C**). Furthermore, GSH not only increased the mitochondrial membrane potential of CP-deficient glioma cells but also effectively inhibited the production of intracellular ROS (**Figure 6D** and **6E**). Western blot analysis showed that the expression of the stress-related proteins ATF4 and CHOP in the ER was significantly decreased

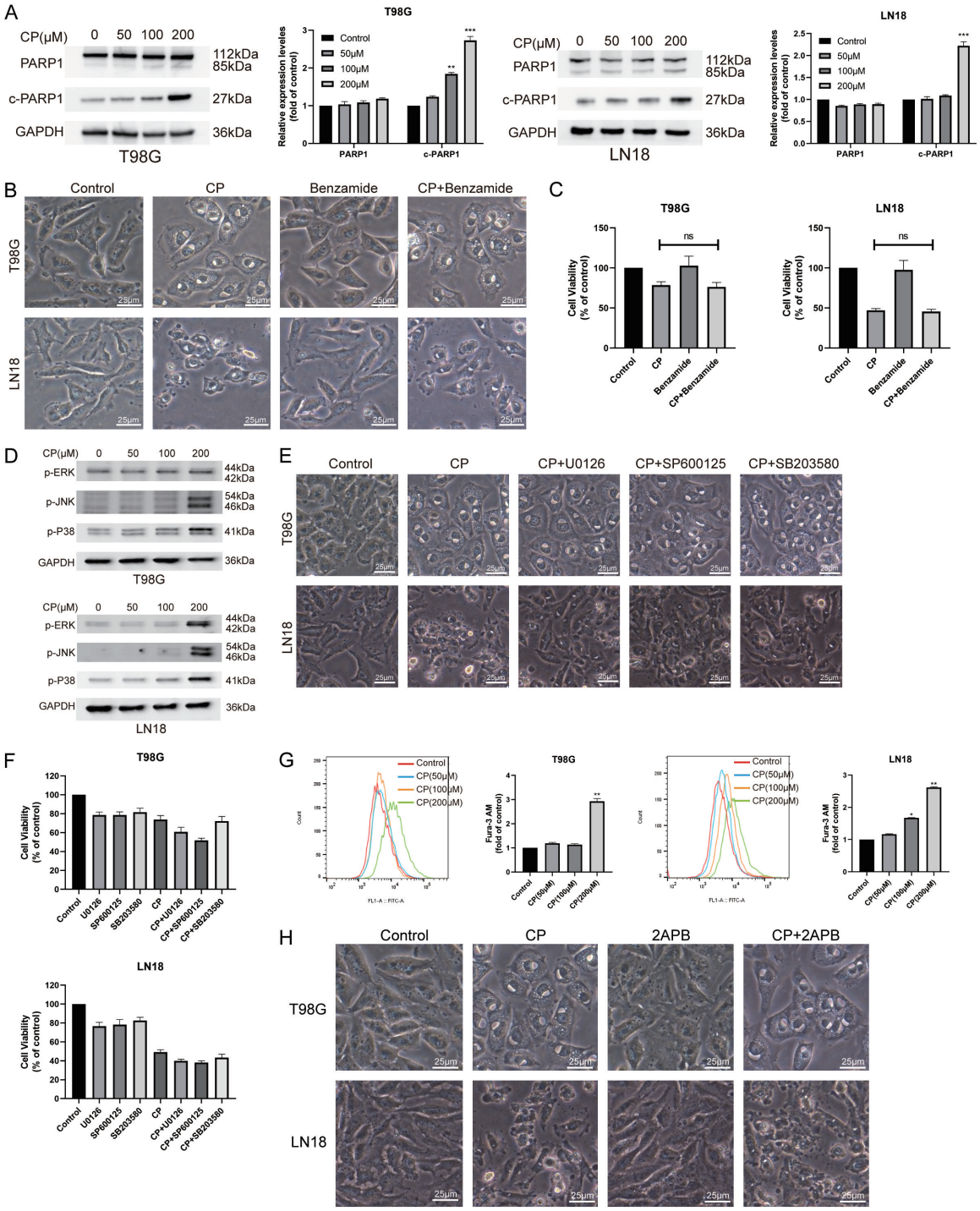

Figure 5. CP activated the PARP1 and MAPK signaling pathways and caused Ca^{2+} overload in glioma cells. A. Western blot analysis of PARP and c-PARP1 in glioma cells. Cells were treated with different concentrations of CP for 6 h (**P < 0.01, ***P < 0.001). B. The effect of the PARP1 inhibitor benzamide (1 mM) on CP-induced cytoplasmic vacuolation. Glioma cells were treated with benzamide (1 mM) and CP (200 μM) for 6 h. C. The effect of benzamide to CP-induced paraptosis. Cells were treated with benzamide (1 mM) and CP (200 μM) for 24 h. The alive cells were measured using CCK-8 assay. D. Western blot analysis of P-ERK, P-JNK, and P-P38 in glioma cells. Cells were treated with different concentrations of CP for 6 h. E. Effects of MAPK signaling pathways inhibitors on CP-induced cytoplasmic vacuolation. Cells were treated with U0126 (20 μM, an ERK inhibitor), SP600125 (20 μM, a JNK inhibitor), SB203580 (20 μM, a p38 inhibitor), and CP (200 μM) for 6 h. F. Effects of MAPK signaling pathways inhibitors to CP-induced paraptosis. Cells were treated with U0126 (20 μM, an ERK inhibitor), SP600125 (20 μM, a JNK inhibitor), SB203580 (20 μM, a p38 inhibitor), and CP (200 μM) for 24 h. The alive cells were measured with a CCK-8 assay. G. After glioma cells were treated with different concentrations of CP for 6 h, intracellular Ca^{2+} levels were analyzed using Fura-3 AM. H. The effects of the IP3R inhibitor 2-APB (20 μM) on CP-induced cytoplasmic vacuolation. Cells were treated with 2-APB (20 μM) and CP (200 μM) for 6 h.

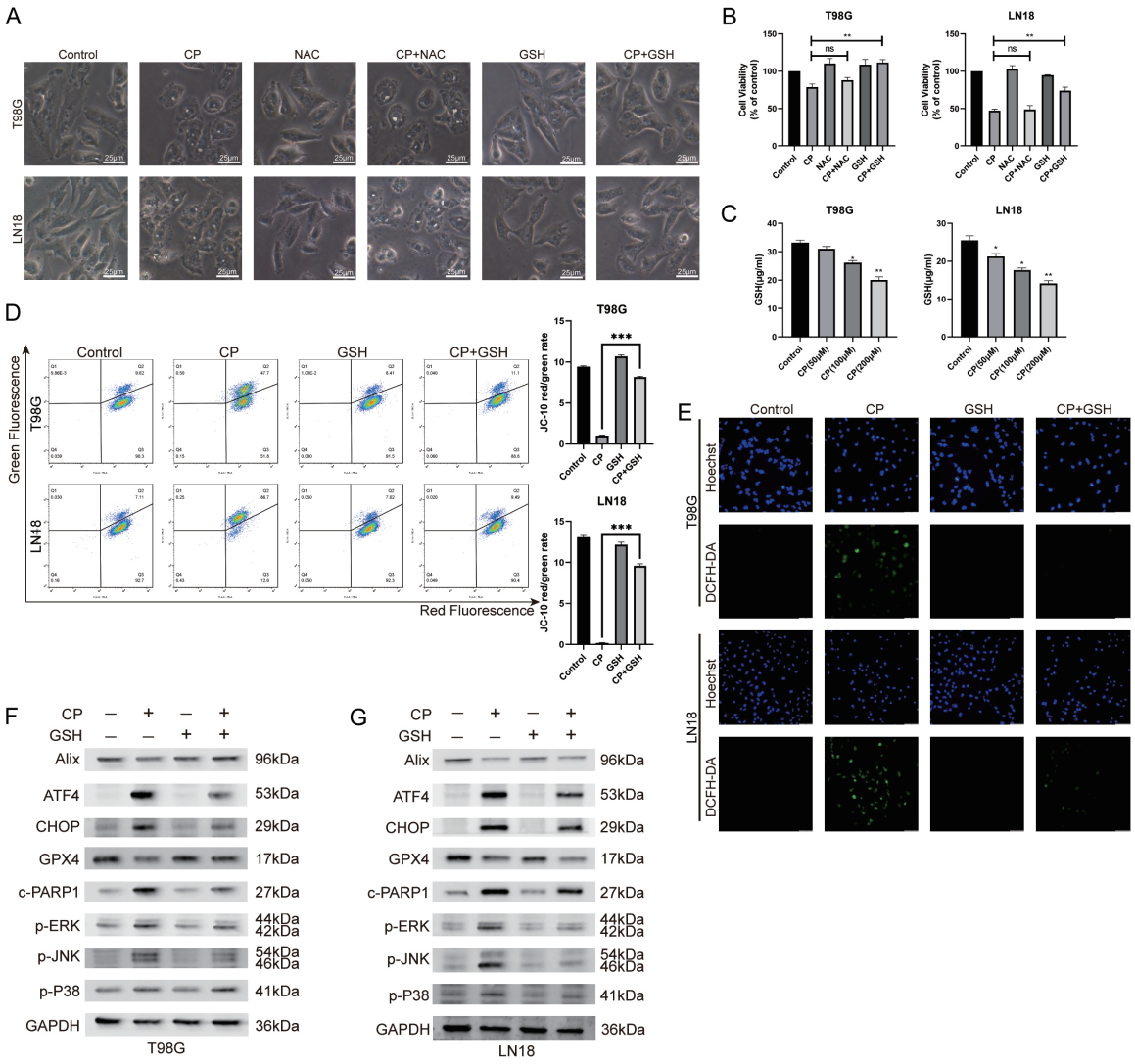

Figure 6. CP inhibited the GSH system in glioma cells. A and B. The effects of NAC (5 mM) and GSH (2 mM) on CP-induced paraptosis. The alive cells were measured with a CCK-8 assay (**P < 0.01). C. CP decreased GSH in glioma cells. Cells were treated with different concentrations of CP for 6 h (**P < 0.01, ***P < 0.001). D and E. GSH blocked CP-induced mitochondrial dysfunction. Cells were treated with GSH (2 mM) and CP (200 μM) for 6 h, and the intracellular ROS levels and mitochondrial membrane potential were detected (***P < 0.001). F and G. GSH blocked CP-induced ER stress and activation of the PARP1 and MAPK pathways. Cells were treated with GSH (2 mM) and CP (200 μM) for 6 h (*P < 0.05, **P < 0.01, ***P < 0.001).

after the addition of GSH. Furthermore, GSH inhibited the activation of the MAPK and PARP1 signaling pathways (**Figure 6F** and **6G**). These results confirmed that GSH-mediated ER stress and mitochondrial dysfunction and that the MAPK and PARP1 signaling pathways were involved in CP-induced paraptosis.

Upregulation of the CHAC1 is critical for the paraptosis induced by CP

In order to explore the molecular mechanism of CP-induced paraptosis in glioma cells, we treated T98G cells with CP and sequenced the transcriptome. The results showed that in the glutathione metabolic pathway, CHAC1 and GCLM were up-regulated, while GGCT, RRM1 and RRM2 were down-regulated (**Figure 7A**). CHAC1 is a member of the protein family encoding γ -glutamyl transferase, which plays a role in regulating glutathione level and oxidative balance in cells. Furthermore, western blot showed that CP increased the expression of CHAC1 in glioma cells (**Figure 7B**). We designed three kinds of siRNA to interfere with the expression of CHAC1 in T98G cells, and chose siCHAC1#1 for

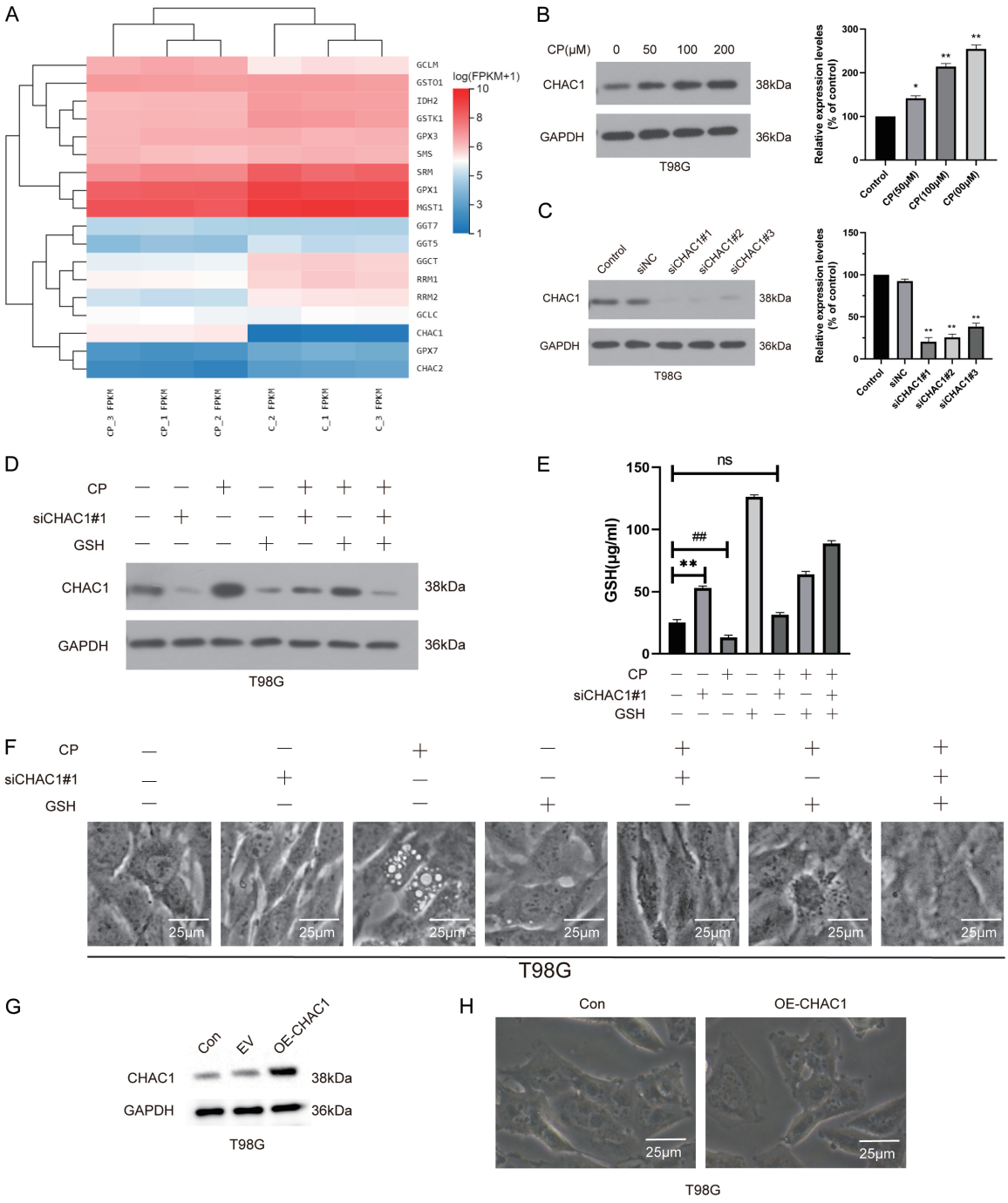

Figure 7. CHAC1 is critical for the paraptosis induced by CP. A. Gene transcription analysis of glutathione metabolic pathway. B. Effect of CP on CHAC1 protein in T98G cells (*P < 0.05, **P < 0.01). C. Changes of CHAC1 protein content in T98G cells treated with siRNA (**P < 0.01). D. Effects of siCHAC1 and GSH on CP-induced changes of CHAC1 protein. E. Effect of siCHAC1 on GSH changes induced by CP (**P < 0.01, ##P < 0.01). F. Microscopic images of T98G cells. The cells were treated with CP (200 μM) combined with or without siCHAC1 or GSH. G. Empty and CHAC1 overexpressing plasmids were transfected into T98G cells. H. Morphological changes of T98G cells after overexpression of CHAC1 plasmid.

the follow-up experiment (**Figure 7C**). Western blot showed that exogenous GSH had no obvious effect on CHAC1 (**Figure 7D**). After interfering with CHAC1, GSH content in glioma cells increased obviously, while CP decreased GSH content in glioma cells, but after treating glio-

ma cells with siCHAC1 and CP at the same time, GSH content in glioma cells did not change significantly (**Figure 7E**). It indicated that CP promoted GSH degradation in glioma cells by up-regulating CHAC1. In addition, interfering with CHAC1 or adding GSH could prevent CP-induced paraptosis (**Figure 7F**). These results indicated that CHAC1 is the critical molecule of CP-induced paraptosis in glioma cells. However, when CHAC1 was overexpressed in T98G cells, no intracellular vacuoles were observed (**Figure 7G**, **7H**).

Discussion

Although glioma treatment has improved in recent years, glioma still has the highest mortality rate among brain tumors [4]. Furthermore, the heterogeneity of glioma facilitates drug resistance and apoptosis evasion, leading to the failure of conventional TMZ treatment [37, 38]. Therefore, it is necessary to identify new therapeutic drugs and develop new therapeutic strategies.

In recent years, natural compounds have been reported to induce paraptosis in cancer cells [8]. Compared to apoptosis, paraptosis is independent of caspase activation, and the caspase inhibitor Z-VAD-FMK cannot prevent paraptosis [23]. CP is a calpain inhibitor with anti-inflammatory and neuroprotective effects [39-41]. CP has also been shown to have anticancer effects in a variety of cancers [19, 20, 22]. In this study, we found that CP induced paraptosis in combination with Alix inhibition in glioma cells. CP induced ER stress and mitochondrial dysfunction, and produced a large amount of intracellular vacuoles. The production of intracellular vacuoles was inhibited by the protein synthesis inhibitor CHX. The antioxidant NAC could not block paraptosis, while GSH could. This finding indicated that oxidative stress was an effect of paraptosis alone, rather than its cause. Destruction of the GSH system is the fundamental reason for CP-induced paraptosis in glioma cells. Furthermore, CP also activated the PARP1, ERK, JNK and P38 pathways, which could also be inhibited by GSH.

The ER is involved in cell protein synthesis, lipid metabolism, and calcium storage [42]. Under stress, the ER can become damaged, leading to a protein folding disorder in the ER and producing a characteristic stress response known as the UPR. Under mild ER stress, the UPR is committed to maintaining endoplasmic reticulum homeostasis. However, when ER stress persists at high levels, the UPR promotes cell death [43, 44]. In this study, we found that CP induced extensive intracellular vacuolation in glioma cells, accompanied by a significant increase in the stress-related proteins ATF4 and CHOP. This finding provided evidence that CP induced ER stress in glioma cells. Furthermore, many studies have shown that MAPK pathway activation and Ca^{2+} overload are involved in paraptosis [28, 33]. Our findings indicated that CP promoted ERK, JNK, and P38 phosphorylation in glioma cells, but the addition of MAPK inhibitors did not prevent cell vacuolation or salvage cell viability. At the same time, CP increased intracellular Ca^{2+} levels, but the addition of the calcium release inhibitor 2-APB also did not prevent paraptosis.

Oxidative stress usually leads to mitochondrial dysfunction. ROS overproduction is involved in various programmed cell death processes. Increased intracellular ROS levels lead to DNA damage, which activates PARP1 signaling [30]. We found that CP induced an increase in ROS levels in glioma cells, decreased mitochondrial membrane potential, and activated the PARP1 pathway. Various natural compounds have been reported to interfere with mitochondrial oxidative phosphorylation in cancer cells and contribute to the appearance of paraptosis [10]. Our results also showed that CP reduced oxidative phosphorylation in glioma cells and reduced ATP production. Furthermore, CP inhibited mPTP opening. Increased mPTP opening promotes apoptosis, but its relationship with paraptosis remains unclear [45]. However, unlike previous studies, we found that the antioxidant NAC did not prevent the generation of intracellular vacuoles. This finding indicated that mitochondrial dysfunction was not the underlying cause of CP-induced paraptosis.

GSH is the most common thiol protein in eukaryotic cells. In addition to its standard antioxidant effects, GSH is also involved in intracellular protein synthesis, DNA synthesis, and other processes [34]. However, in some cancer cells, increased levels of GSH are related to cancer progression and promotion of drug resistance [35]. GSH in the ER is involved in protein folding, translocation, glycosylation,

and disulfide bond formation. The synthesis of disulfide bonds is the main factor in protein folding [46]. It has been shown to be involved in various cell death processes, including apoptosis, necrosis, and ferroptosis [36]. CHAC1 is a member of the protein family encoding γ -glutamyl transferase, which plays a role in regulating GSH level and oxidative balance in cells [15]. The latest research suggests that GSH degradation mediated by CHAC1 contributes to auranofin-induced paraptosis in breast cancer cells [47]. In this study, we showed that CP reduced the GSH content in glioma cells, while GSH could block CP-induced paraptosis. GSH also reduced intracellular ROS levels, restored mitochondrial membrane potential, inhibited the activation of MAPK and PARP proteins, and reduced ATF4 and CHOP protein levels, thus inhibiting ER stress and restoring mitochondrial function. Furthermore, Anupama Binoy et al. found that plumbagin could induce paraptosis by changing sulfhydryl homeostasis in cells, and the thiol antioxidant NAC could completely reverse the effect of plumbagin [48]. In our study, it was found that NAC could not prevent CP-induced paraptosis, so we believed there was no direct relationship between changes in sulfhydryl homeostasis and CP-induced paraptosis. Transcriptome sequencing results showed that CP upregulated the transcription of CHAC1, and western blot also showed that CP promoted the expression of CHAC1 protein. After CHAC1 was knocked out, GSH content in glioma cells increased significantly. Most importantly, knocking out CHAC1 could prevent CP-induced paraptosis. However, our experiments demonstrated that transient overexpression of CHAC1 in T98G cells did not produce obvious cytoplasmic vacuoles. This result does not contradict our conclusion but rather suggests that CHAC1-mediated GSH degradation is necessary yet not sufficient to trigger the full paraptotic phenotype. The failure of single-gene CHAC1 overexpression to form vacuoles underscores that CP-induced paraptosis is a systems-level response.

Conclusions

In summary, the findings of our study showed that CP induced ER stress and mitochondrial dysfunction in glioma cells by the degradation of GSH mediated by CHAC1, and CHAC1 is a key molecule in CP-induced paraptosis of glioma cells. The ability of CP to induce paraptosis in glioma cells suggests that CP is a promising anticancer drug.

Acknowledgements

This work was supported by Natural Science Foundation of Henan Province (222300420359), Medical Science and Technology Research Plan of Henan Province (SBGJ202103015), Scientific Reuter Foundation of Jilin Province (20200201613JC, and 20200201388JC), Training Project of Young and Middle-aged Health Science and Technology Innovation Leading Talents in Henan Province (YXKC2021004).

Disclosure of conflict of interest

None.

Abbreviations

2-APB, 2-Aminoethyl Diphenylborinate; 4-PBA, 4-Phenylbutyric acid; Alix, Alg-2 interacting protein X; ATF4, Activating transcription factor 4; CCK-8, cell counting kit-8; CHAC1, Cation transport regulator homolog-1; CHX, cycloheximide; CP, calpeptin; DMEM, Dulbecco's modified Eagle's medium; ER, endoplasmic reticulum; FBS, Fetal bovine serum; GSH, glutathione; MAPK, mitogen-activated protein kinase; mPTP, mitochondrial permeability transition pore; NAC, N-acetylcysteine; OCR, oxygen consumption rate; PI, propidium iodide; ROS, reactive oxygen species; TEM, transmission electron microscopy; TMZ, temozolomide; UPR, unfolded protein response.

Address correspondence to: Dr. Ziqiang Liu and Chaoyue Li, Henan Provincial People's Hospital, Cerebrovascular Disease Hospital, People's Hospital of Zhengzhou University, No. 7, Weiwu Road, Zhengzhou 450003, Henan, China. Tel: +86-15737160251; E-mail: ziqiang19@mails.jlu.edu.cn (ZQL); Tel: +86-13676976929; E-mail: lichaoyue@zzu.edu.cn (CYL)

References

[1] Wang Y, Wang Y, Bao H, Wang Z and Jiang T. Mechanisms and therapeutic implications of glioma-neuron interactions. Cancer Lett 2025; 629: 217884.

[2] Sung H, Ferlay J, Siegel RL, Laversanne M, Soerjomataram I, Jemal A and Bray F. Global

cancer statistics 2020: GLOBOCAN estimates of incidence and mortality worldwide for 36 cancers in 185 countries. CA Cancer J Clin 2021; 71: 209-249.
[3] Ostrom QT, Gittleman H, Farah P, Ondracek A, Chen Y, Wolinsky Y, Stroup NE, Kruchko C and Barnholtz-Sloan JS. CBTRUS statistical report: Primary brain and central nervous system tumors diagnosed in the United States in 2006-2010. Neuro Oncol 2013; 15 Suppl 2: ii1-56.
[4] Ostrom QT, Bauchet L, Davis FG, Deltour I, Fisher JL, Langer CE, Pekmezci M, Schwartzbaum JA, Turner MC, Walsh KM, Wrensch MR and Barnholtz-Sloan JS. The epidemiology of glioma in adults: a "state of the science" review. Neuro Oncol 2014; 16: 896-913.
[5] Monje M. The neuroscience of brain cancers. Neuron 2025; 113: 2734-2739.
[6] Li H, Wu Y, Chen Y, Lv J, Qu C, Mei T, Zheng Y, Ye C, Li F, Ge S, Yao A and Jia L. Overcoming temozolomide resistance in glioma: recent advances and mechanistic insights. Acta Neuropathol Commun 2025; 13: 126.
[7] Sperandio S, de Belle I and Bredesen DE. An alternative, nonapoptotic form of programmed cell death. Proc Natl Acad Sci U S A 2000; 97: 14376-14381.
[8] Lee D, Kim IY, Saha S and Choi KS. Paraptosis in the anti-cancer arsenal of natural products. Pharmacol Ther 2016; 162: 120-133.
[9] Liu X, Gu Y, Bian Y, Cai D, Li Y, Zhao Y, Zhang Z, Xue M and Zhang L. Honokiol induces paraptosis-like cell death of acute promyelocytic leukemia via mTOR & MAPK signaling pathways activation. Apoptosis 2021; 26: 195-208.
[10] Wang Y, Wen X, Zhang N, Wang L, Hao D, Jiang X and He G. Small-molecule compounds target paraptosis to improve cancer therapy. Biomed Pharmacother 2019; 118: 109203.
[11] Anceschi C, Frediani E, Ruzzolini J, Margheri F, Chillà A, Formica N, Andreucci E, Cianchi F, Laurenzana A and Martinelli S. Die hard: when cells refuse apoptosis-the rise of paraptosis and other death pathways. Cell Death Discov 2026; [Epub ahead of print].
[12] Sang J, Li W, Diao HJ, Fan RZ, Huang JL, Gan L, Zou MF, Tang GH and Yin S. Jolkinolide B targets thioredoxin and glutathione systems to induce ROS-mediated paraptosis and apoptosis in bladder cancer cells. Cancer Lett 2021; 509: 13-25.
[13] Gargalovic PS, Imura M, Zhang B, Gharavi NM, Clark MJ, Pagnon J, Yang WP, He A, Truong A, Patel S, Nelson SF, Horvath S, Berliner JA, Kirchgessner TG and Lusis AJ. Identification of inflammatory gene modules based on variations of human endothelial cell responses to oxidized lipids. Proc Natl Acad Sci U S A 2006; 103: 12741-12746.
[14] Mungrue IN, Pagnon J, Kohannim O, Gargalovic PS and Lusis AJ. CHAC1/MGC4504 is a novel proapoptotic component of the unfolded protein response, downstream of the ATF4-ATF3-CHOP cascade. J Immunol 2009; 182: 466-476.
[15] Chen MS, Wang SF, Hsu CY, Yin PH, Yeh TS, Lee HC and Tseng LM. CHAC1 degradation of glutathione enhances cystine-starvation-induced necroptosis and ferroptosis in human triple negative breast cancer cells via the GCN2-eIF2α-ATF4 pathway. Oncotarget 2017; 8: 114588-114602.
[16] Zhou Z and Zhang H. CHAC1 exacerbates LPS-induced ferroptosis and apoptosis in HK-2 cells by promoting oxidative stress. Allergol Immunopathol (Madr) 2023; 51: 99-110.
[17] Wang N, Zeng GZ, Yin JL and Bian ZX. Artesunate activates the ATF4-CHOP-CHAC1 pathway and affects ferroptosis in Burkitt's Lymphoma. Biochem Biophys Res Commun 2019; 519: 533-539.
[18] Ge Y, Zheng X, Mao S, Zhang Q, Hu G and Wei Y. DJ-1 inhibits glutathione degradation by downregulating CHAC1 expression in astrocytes. Neurosci Res 2022; 184: 62-69.
[19] Yoshida M, Miyasaka Y, Ohuchida K, Okumura T, Zheng B, Torata N, Fujita H, Nabae T, Manabe T, Shimamoto M, Ohtsuka T, Mizumoto K and Nakamura M. Calpain inhibitor calpeptin suppresses pancreatic cancer by disrupting cancer-stromal interactions in a mouse xenograft model. Cancer Sci 2016; 107: 1443-1452.
[20] Mataga MA, Rosenthal S, Heerboth S, Devalapalli A, Kokolus S, Evans LR, Longacre M, Housman G and Sarkar S. Anti-breast cancer effects of histone deacetylase inhibitors and calpain inhibitor. Anticancer Res 2012; 32: 2523-2529.
[21] Sundaramoorthy P, Sim JJ, Jang YS, Mishra SK, Jeong KY, Mander P, Chul OB, Shim WS, Oh SH, Nam KY and Kim HM. Modulation of intracellular calcium levels by calcium lactate affects colon cancer cell motility through calcium-dependent calpain. PLoS One 2015; 10: e0116984.
[22] Cai L, Li Q, Li W, Wang C, Tu M, Zhu Z, Su Z and Lu X. Calpain suppresses cell growth and invasion of glioblastoma multiforme by producing the cleavage of filamin A. Int J Clin Oncol 2020; 25: 1055-1066.
[23] Fontana F, Raimondi M, Marzagalli M, Di Domizio A and Limonta P. The emerging role of paraptosis in tumor cell biology: Perspectives for cancer prevention and therapy with natural compounds. Biochim Biophys Acta Rev Cancer 2020; 1873: 188338.
[24] Sperandio S, Poksay K, de Belle I, Lafuente MJ, Liu B, Nasir J and Bredesen DE. Paraptosis:

mediation by MAP kinases and inhibition by AIP-1/Alix. Cell Death Differ 2004; 11: 1066-1075.
[25] Solovieva M, Shatalin Y, Fadeev R, Krestinina O, Baburina Y, Kruglov A, Kharechkina E, Kobyakova M, Rogachevsky V, Shishkova E and Akatov AV. Vitamin B12b enhances the cytotoxicity of diethyldithiocarbamate in a synergistic manner, inducing the paraptosis-like death of human larynx carcinoma cells. Biomolecules 2020; 10: 69.
[26] Chen X, Chen X, Zhang X, Wang L, Cao P, Rajamanickam V, Wu C, Zhou H, Cai Y, Liang G and Wang Y. Curcuminoid B63 induces ROS-mediated paraptosis-like cell death by targeting TrxR1 in gastric cells. Redox Biol 2019; 21: 101061.
[27] Kar R, Singha PK, Venkatachalam MA and Saikumar P. A novel role for MAP1 LC3 in non-autophagic cytoplasmic vacuolation death of cancer cells. Oncogene 2009; 28: 2556-2568.
[28] Guamán-Ortiz LM, Orellana MI and Ratovitski EA. Natural compounds as modulators of non-apoptotic cell death in cancer cells. Curr Genomics 2017; 18: 132-155.
[29] Zhu D, Chen C, Xia Y, Kong LY and Luo J. A purified resin glycoside fraction from pharbitidis semen induces paraptosis by activating chloride intracellular channel-1 in human colon cancer cells. Integr Cancer Ther 2019; 18: 1534735418822120.
[30] Mir H, Rajawat J, Vohra I, Vaishnav J, Kadam A and Begum R. Signaling interplay between PARP1 and ROS regulates stress-induced cell death and developmental changes in Dictyostelium discoideum. Exp Cell Res 2020; 397: 112364.
[31] Boyman L, Karbowski M and Lederer WJ. Regulation of mitochondrial ATP production: Ca^{2+} signaling and quality control. Trends Mol Med 2020; 26: 21-39.
[32] Lee AR, Seo MJ, Kim J, Lee DM, Kim IY, Yoon MJ, Hoon H and Choi KS. Lercanidipine synergistically enhances bortezomib cytotoxicity in cancer cells via enhanced endoplasmic reticulum stress and mitochondrial Ca^{2+} overload. Int J Mol Sci 2019; 20: 6112.
[33] Kim E, Lee DM, Seo MJ, Lee HJ and Choi KS. Intracellular Ca2+ imbalance critically contributes to paraptosis. Front Cell Dev Biol 2020; 8: 607844.
[34] Bansal A and Simon MC. Glutathione metabolism in cancer progression and treatment resistance. J Cell Biol 2018; 217: 2291-2298.
[35] Kennedy L, Sandhu JK, Harper ME and Cuperlovic-Culf M. Role of glutathione in cancer: from mechanisms to therapies. Biomolecules 2020; 10: 1429.
[36] Lv H, Zhen C, Liu J, Yang P, Hu L and Shang P. Unraveling the potential role of glutathione in multiple forms of cell death in cancer therapy. Oxid Med Cell Longev 2019; 2019: 3150145.
[37] Mittelbronn M, Platten M, Zeiner P, Dombrowski Y, Frank B, Zachskorn C, Harter PN, Weller M and Wischhusen J. Macrophage migration inhibitory factor (MIF) expression in human malignant gliomas contributes to immune escape and tumour progression. Acta Neuropathol 2011; 122: 353-365.
[38] Cong D, Zhu W, Shi Y, Pointer KB, Clark PA, Shen H, Kuo JS, Hu S and Sun D. Upregulation of NHE1 protein expression enables glioblastoma cells to escape TMZ-mediated toxicity via increased H^+ extrusion, cell migration and survival. Carcinogenesis 2014; 35: 2014-2024.
[39] Su B, Guan Q, Wang M, Liu N, Wei X, Wang S, Yang X, Jiang W, Xu M and Yu S. Calpeptin is neuroprotective against acrylamide-induced neuropathy in rats. Toxicology 2018; 400-401: 1-8.
[40] Song ZJ, Yang SJ, Han L, Wang B and Zhu G. Postnatal calpeptin treatment causes hippocampal neurodevelopmental defects in neonatal rats. Neural Regen Res 2019; 14: 834-840.
[41] Zuo J, Hu Z, Liu T, Chen C, Tao Z, Chen S and Li F. Calpeptin attenuates cigarette smoke-induced pulmonary inflammation via suppressing calpain/IκBα signaling in mice and BEAS-2B cells. Pathol Res Pract 2018; 214: 1199-1209.
[42] Schwarz DS and Blower MD. The endoplasmic reticulum: structure, function and response to cellular signaling. Cell Mol Life Sci 2016; 73: 79-94.
[43] Oakes SA and Papa FR. The role of endoplasmic reticulum stress in human pathology. Annu Rev Pathol 2015; 10: 173-194.
[44] Oakes SA. Endoplasmic reticulum stress signaling in cancer cells. Am J Pathol 2020; 190: 934-946.
[45] Huo H, Zhou Z, Qin J, Liu W, Wang B and Gu Y. Erastin disrupts mitochondrial permeability transition Pore (mPTP) and induces apoptotic death of colorectal cancer cells. PLoS One 2016; 11: e0154605.
[46] Wang M and Kaufman RJ. Protein misfolding in the endoplasmic reticulum as a conduit to human disease. Nature 2016; 529: 326-335.
[47] Seo MJ, Kim IY, Lee DM, Park YJ, Cho MY, Jin HJ and Choi KS. Dual inhibition of thioredoxin reductase and proteasome is required for auranofin-induced paraptosis in breast cancer cells. Cell Death Dis 2023; 14: 42.
[48] Binoy A, Nedungadi D, Katiyar N, Bose C, Shankarappa SA, Nair BG and Mishra N. Plumbagin induces paraptosis in cancer cells by disrupting the sulfhydryl homeostasis and proteasomal function. Chem Biol Interact 2019; 310: 108733.